Functionalization of Micelles and Shell Cross-linked Nanoparticles Using Click Chemistry

Rachel K. O'Reilly,[†,‡] Maisie J. Joralemon,[†] Karen L. Wooley,*[,†] and Craig J. Hawker*[,‡,§]

Center for Materials Innovation and Department of Chemistry, Washington University in Saint Louis, One Brookings Drive, Saint Louis, Missouri 63130-4899, IBM Almaden Research Center, 650 Harry Road, San Jose, California 95120, and Materials Research Laboratory, University of California, Santa Barbara, California 93106

Received May 17, 2005. Revised Manuscript Received September 16, 2005

Shell cross-linked nanoparticles (SCKs) presenting Click-reactive functional groups in either the hydrophilic shell or the hydrophobic core region of block copolymer micelles in aqueous solution were synthesized by two routes. The first route utilized amidation chemistry to functionalize poly(acrylic acid) within the micelle shell with either azido or alkynyl groups. The second route employed latent functionality to introduce azido groups into the polystyrene core of the micelles. These Click-functionalized micelles were then cross-linked in an intramicellar fashion via amidation reactions within the shell layer to afford the SCKs bearing alkynyl groups in the shell or azido in the shell or core domains. The availability and reactivity of the functional groups in these nanoparticles toward Click chemistry was demonstrated by reaction with complementary Click-functionalized fluorescent dyes. The hydrodynamic diameters (D_h) of the micelles and nanoparticles were typically ca. 25 nm, as determined by dynamic light scattering. The dimensions of the nanoparticles were also characterized as deposited on substrates using tapping-mode atomic force microscopy to obtain the heights and transmission electron microscopy for measurement of the diameters. Studies by analytical ultracentrifugation sedimentation equilibrium equipped with UV−vis detection optics confirmed the covalent attachment of the fluorescent tags in the core or shell region of the nanoparticles.

Introduction

Well-defined nanostructured materials have attracted considerable interest over the past decade, due to the unique behaviors of nanoscale objects that can be exploited in a wide range of applications such as in environmental and materials sciences and in biomedicine.[1−7] As a result, the development of methodologies for their preparation and examination of their properties has received much study.[8−16] Perhaps the most universal technique for the preparation of nanoparticles having controlled morphologies is the self-assembly of amphiphilic block copolymers in selective solvents, to afford polymer micelles or vesicles.[17−20] These polymeric micelles can then be transformed into robust amphiphilic nanoscale particles with well-defined core−shell morphologies via covalent cross-linking, in either the core[21] or shell[22−26] domains. With limitation of the cross-links to the polymer chain segments that compose the peripheral

* Corresponding authors. E-mail: hawker@mrl.ucsb.edu; klwooley@artsci.wustl.edu.
† Washington University in Saint Louis.
‡ IBM Almaden Research Center.
§ University of California, Santa Barbara.

(1) (a) Larson, D. R.; Zipfel, W. R.; Williams, R. M.; Clark, S. W.; Bruchez, M. P.; Wise, F. W.; Webb, W. W. *Science* **2003**, *300*, 1434−1436. (b) Hawker, C. J.; Wooley, K. L *Science*, **2005**, *309*, 1200−1205.
(2) Gillies, E. R.; Fréchet, J. M. J. *J. Am. Chem. Soc.* **2002**, *124*, 14137−14146.
(3) Moses, M. A.; Brem, H.; Langer, R. *Cancer Cell* **2003**, *4*, 337−341.
(4) Becker, M. L.; Bailey, L. O.; Wooley, K. L. *Bioconjugate Chem.* **2004**, *15*, 710−717.
(5) Bae, Y.; Nishiyama, N.; Fukushima, S.; Koyama, H.; Yasuhiro, M.; Kataoka, K. *Bioconjugate Chem.* **2005**, *16*, 122−130.
(6) Wathier, M.; Jung, P. J.; Carnahan, M. A.; Kim, T.; Grinstaff, M. W. *J. Am. Chem. Soc.* **2004**, *126*, 12744−12745.
(7) Vutukuri, D. R.; Basu, S.; Thayumanavan, S. *J. Am. Chem. Soc.* **2004**, *126*, 15636−15637.
(8) Butun, V.; Lowe, A. B.; Billingham, N. C.; Armes, S. P. *J. Am. Chem. Soc.* **1999**, *121*, 4288−4289.
(9) Bosman, A. W.; Vestberg, R.; Heumann, A.; Fréchet, J. M. J.; Hawker, C. J. *J. Am. Chem. Soc.* **2003**, *125*, 715−728.
(10) Becker, M. L.; Liu, J. Q.; Wooley, K. L. *Biomacromolecules* **2005**, *6*, 220−228.
(11) Kang, Y.; Taton, T. A. *Angew. Chem., Int. Ed.* **2005**, *44*, 409−412.
(12) Li, Z.; Kesselman, E.; Talmon, Y.; Hillmyer, M. A.; Lodge, T. P. *Science* **2004**, *306*, 98−101.
(13) Pochan, D. J.; Chen, Z.; Cui, H.; Hales, K.; Qi, K.; Wooley, K. L. *Science* **2004**, *306*, 94−97.
(14) Stupp, S. I.; Beniash, E.; Hartgerink, J. D.; Sone, E. D. *Bio-Implant Interface* **2003**, 393−406.
(15) Vriezema, D. M.; Aragones, M. C.; Elemans, J. A. A. W.; Cornelissen, J. J. L. M.; Rowan, A. E.; Nolte, R. J. M. *Chem. Rev.* **2005**, *105*, 1445−1489.
(16) Hoeben, F. J. M.; Jonkheijm, P.; Meijer, E. W.; Schenning, A. P. H. J. *Chem. Rev.* **2005**, *105*, 1491−1546.
(17) Matejicek, P.; Uhlik, F.; Limpouchova, Z.; Prochazka, K.; Tuzar, Z.; Webber, S. E. *Macromolecules* **2002**, *35*, 9487−9496.
(18) Gillies, E. R.; Fréchet, J. M. J. *Chem. Commun.* **2003**, 1640−1641.
(19) Choucair, A.; Lavigueur, C.; Eisenberg, A. *Langmuir* **2004**, *20*, 3894−3900.
(20) Discher, D. E.; Eisenberg, A. *Science* **2002**, *297*, 967−973.
(21) Loppinet, B.; Sigel, R.; Larsen, A.; Fytas, G.; Vlassopoulos, D.; Liu, G. *Langmuir* **2000**, *16*, 6480−6484.
(22) Henselwood, F.; Liu, G. J. *Macromolecules* **1997**, *30*, 488−493.
(23) Thurmond, K. B., II; Kowalewski, T.; Wooley, K. L. *J. Am. Chem. Soc.* **1996**, *118*, 7239−7240.
(24) Butun, V.; Billingham, N. C.; Armes, S. P. *J. Am. Chem. Soc.* **1998**, *120*, 12135−12136.
(25) Discher, B. M.; Won, Y. Y.; Ege, D. S.; Lee, J. C. M.; Bates, F. S.; Discher, D. E.; Hammer, D. A. *Science* **1999**, *284*, 1143−1146.
(26) Sanji, T.; Nakatsuka, Y.; Kitayama, F.; Sakurai, H. *Chem. Commun.* **1999**, 2201−2202.

10.1021/cm051047s CCC: $30.25
Published on Web 10/28/2005

micelle shell, shell cross-linked knedel-like nanoparticles (SCKs) can be formed, which consist of a hydrophobic core domain and a cross-linked hydrophilic shell layer.[23] Our interest is primarily focused on these amphiphilic nanostructures, due to their analogy to biological constructs.[27]

SCKs have been demonstrated to be stable,[28] biocompatible,[4] and capable of hydrophobic guest sequestration and transport,[29,30] in analogy with lipoproteins. Recent synthetic advances in living free radical polymerization techniques[31−34] have allowed for the preparation of a wide range of well-defined block copolymers, thus affording readily tunable structural and chemical features of the nanoparticles. Indeed, the ability to control the dimensions, morphology, and composition of these nanoparticles is important.[19]

The functionalization and tailoring of the SCK shell has been reported to present molecular recognition elements on the nanoparticle surface.[35] Furthermore, there has been ever-growing interest in the bioconjugation of nanoparticles,[36,37] to allow the attachment and surface presentation of ligands for complexation and coordination, for applications in biomimetics, targeted delivery, and biodetection.[38−44] It has been shown that these nanoparticles can be surface-conjugated with mannose,[45] folate,[46] peptides,[47] and other moieties.[48] Two primary synthetic strategies for this functionalization have been established for the preparation of these materials and involve either use of a functionalized initiator species[10,45] together with a mixed-micelle assembly or a secondary functionalization step after establishment of the nanoparticle, involving the same amidation chemistry that was used to construct the cross-linked shell.[46,47]

In an effort to broaden the range of amphiphilic nanoparticle functionalization reactions and increase their selectivity, the synthesis and characterization of SCKs incorporating specific functional groups in the shell or core domain is reported, followed by their use as chemically distinct sites onto which unique functional groups can be attached. Ultimately, the intended application of these functionalized nanoparticles in the study of biological processes depends on two key factors, orthogonality and selectivity in the relevant physiological settings.[49] It has been shown that the stability of azides and alkynes in aqueous solutions and their unreactive nature toward biological molecules enables these functionalities to behave as inert chemical handles for a diverse set of selective chemical reactions,[50] for example, the highly efficient copper(I)-catalyzed Huisgen 1,3-dipolar cycloaddition between azides and terminal alkynes[51] to regiospecifically form 1,2,3-triazoles.[52,53] This quantitative "Click" reaction has recently been utilized in a wide range of applications: in the functionalization[54−56] and synthesis of polymers,[57,58] small molecules,[59,60] and biomolecules,[61−66] in the functionalization of surfaces,[67−70] in the synthesis of dendrimers (both divergently[71] and convergently[72]), as a probe in biological systems,[73−76] in the building of libraries,[77−79]

(27) Wooley, K. L. *J. Polym. Sci., Part A: Polym. Chem.* **2000**, *38*, 1397−1407.
(28) Huang, H. Y.; Remsen, E. E.; Kowalewski, T.; Wooley, K. L. *J. Am. Chem. Soc.* **1999**, *121*, 3805−3806.
(29) Kao, H. M.; O'Connor, R. D.; Mehta, A. K.; Huang, H. Y.; Poliks, B.; Wooley, K. L.; Schaefer, J. *Macromolecules* **2001**, *34*, 544−546.
(30) Turner, J. L.; Wooley, K. L. *Nano Lett.* **2004**, *4*, 683−688.
(31) Matyjaszewski, K.; Xia, J. H. *Chem. Rev.* **2001**, *101*, 2921−2990.
(32) Kamigaito, M.; Ando, T.; Sawamoto, M. *Chem. Rev.* **2001**, *101*, 3689−3745.
(33) Hawker, C. J.; Bosman, A. W.; Harth, E. *Chem. Rev.* **2001**, *101*, 3661−3688.
(34) Chiefari, J.; Chong, Y. K.; Ercole, F.; Krstina, J.; Jeffery, J.; Le, T. P. T.; Mayadunne, R. T. A.; Meijs, G. F.; Moad, C. L.; Moad, G.; Rizzardo, E.; Thang, S. H. *Macromolecules* **1998**, *31*, 5559−5562.
(35) Narain, R.; Armes, S. P. *Biomacromolecules* **2003**, *4*, 1746−1758.
(36) Niemeyer, C. M. *Angew. Chem., Int. Ed.* **2001**, *40*, 4128−4158.
(37) Narain, R.; Armes, S. P. *Macromolecules* **2003**, *36*, 4675−4678.
(38) Sarikaya, M.; Tamerler, C.; Jen, A. K. Y.; Schulten, K.; Baneyx, F. *Nat. Mater.* **2003**, *2*, 577−585.
(39) Mann, S. *Angew. Chem., Int. Ed.* **2000**, *39*, 3393−3406.
(40) Berry, C. C.; Curtis, A. S. G. *J. Phys. D: Appl. Phys.* **2003**, *36*, R198−R206.
(41) Kakizawa, Y.; Kataoka, K. *Adv. Drug Delivery Rev.* **2002**, *54*, 203−222.
(42) Langer, R. *Science* **2001**, *293*, 58−59.
(43) Nam, J. M.; Thaxton, C. S.; Mirkin, C. A. *Science* **2003**, *301*, 1884−1886.
(44) Verma, A.; Rotello, V. M. *Chem. Commun.* **2005**, 303−312.
(45) Joralemon, M. J.; Murthy, K. S.; Remsen, E. E.; Becker, M. L.; Wooley, K. L. *Biomacromolecules* **2004**, *5*, 903−913.
(46) Pan, D.; Turner, J. L.; Wooley, K. L. *Chem. Commun.* **2003**, 2400−2401.
(47) Becker, M. L.; Remsen, E. E.; Pan, D.; Wooley, K. L. *Bioconjugate Chem.* **2004**, *15*, 699−709.
(48) Pan, D. J.; Turner, J. L.; Wooley, K. L. *Macromolecules* **2004**, *37*, 7109−7115.
(49) Kolb, H. C.; Sharpless, K. B. *Drug Discovery Today* **2003**, *8*, 1128−1137.
(50) Köhn, M.; Breinbauer, R. *Angew. Chem., Int. Ed.* **2004**, *43*, 3106−3116.
(51) Huisgen, R. *Angew. Chem., Int. Ed.* **1968**, *7*, 321−328.
(52) Tornoe, C. W.; Christensen, C.; Meldal, M. *J. Org. Chem.* **2002**, *67*, 3057−3064.
(53) Chan, T. R.; Hilgraf, R.; Sharpless, K. B.; Fokin, V. V. *Org. Lett.* **2004**, *6*, 2853−2855.
(54) Binder, W. H.; Kluger, C. *Macromolecules* **2004**, *37*, 9321−9330.
(55) Helms, B.; Mynar, J. L.; Hawker, C. J.; Fréchet, J. M. J. *J. Am. Chem. Soc.* **2004**, *126*, 15020−15021.
(56) Tsarevsky, N. V.; Bernaerts, K. V.; Dufour, B.; Du Prez, F. E.; Matyjaszewski, K. *Macromolecules* **2004**, *37*, 9308−9313.
(57) Diaz, D. D.; Punna, S.; Holzer, P.; McPherson, A. K.; Sharpless, K. B.; Fokin, V. V.; Finn, M. G. *J. Polym. Sci., Part A: Polym. Chem.* **2004**, *42*, 4392−4403.
(58) Opsteen, J. A.; van Hest, J. C. M. *Chem. Commun.* **2005**, 57−59.
(59) Bodine, K. D.; Gin, D. Y.; Gin, M. S. *J. Am. Chem. Soc.* **2004**, *126*, 1638−1639.
(60) Shintani, R.; Fu, G. C. *J. Am. Chem. Soc.* **2003**, *125*, 10778−10779.
(61) Mocharla, V. P.; Colasson, B.; Lee, L. V.; Roper, S.; Sharpless, K. B.; Wong, C. H.; Kolb, H. C. *Angew. Chem., Int. Ed.* **2005**, *44*, 116−120.
(62) Kuijpers, B. H. M.; Groothuys, S.; Keereweer, A. R.; Quaedflieg, P. J. L. M.; Blaauw, R. H.; van Delft, F. L.; Rutjes, F., P. J. T. *Org. Lett.* **2004**, *6*, 3123−3126.
(63) Suh, B.-C.; Jeon, H.; Posner, G. H.; Silverman, S. M. *Tetrahedron Lett.* **2004**, *45*, 4623−4625.
(64) Adam, G. C.; Vanderwal, C. D.; Sorensen, E. J.; Cravatt, B. F. *Angew. Chem., Int. Ed.* **2003**, *42*, 5480−5484.
(65) Fu, X.; Albermann, C.; Jiang, J. Q.; Liao, J. C.; Zhang, C. S.; Thorson, J. S. *Nat. Biotechnol.* **2003**, *21*, 1467−1469.
(66) Perez-Balderas, F.; Ortega-Munoz, M.; Morales-Sanfrutos, J.; Hernandez-Mateo, F.; Calvo-Flores, F. G.; Calvo-Asin, J. A.; Isac-Garcia, J.; Santoyo-Gonzalez, F. *Org. Lett.* **2003**, *5*, 1951−1954.
(67) Collman, J. P.; Devaraj, N. K.; Chidsey, C. E. D. *Langmuir* **2004**, *20*, 1051−1053.
(68) Lummerstorfer, T.; Hoffmann, H. *J. Phys. Chem. B* **2004**, *108*, 3963−3966.
(69) Lee, J. K.; Chi, Y. S.; Choi, I. S. *Langmuir* **2004**, *20*, 3844−3847.
(70) Link, A. J.; Tirrell, D. A. *J. Am. Chem. Soc.* **2003**, *125*, 11164−11165.
(71) Joralemon, M. J.; O'reilly, R. K.; Matson, J. B.; Nugent, A. K.; Hawker, C. J.; Wooley, K. L. *Macromolecules* **2005**, *38*, 5436−5443.
(72) Wu, P.; Feldman, A. K.; Nugent, A. K.; Hawker, C. J.; Scheel, A.; Voit, B.; Pyun, J.; Fréchet, J. M. J.; Sharpless, K. B.; Fokin, V. V. *Angew. Chem., Int. Ed.* **2004**, *43*, 3928−3932.
(73) Speers, A. E.; Cravatt, B. F. *Chem. Biol.* **2004**, *11*, 535−546.
(74) Seo, T. S.; Li, Z. M.; Ruparel, H.; Ju, J. Y. *J. Org. Chem.* **2003**, *68*, 609−612.
(75) Manetsch, R.; Krasinski, A.; Radic, Z.; Raushel, J.; Taylor, P.; Sharpless, K. B.; Kolb, H. C. *J. Am. Chem. Soc.* **2004**, *126*, 12809−12818.

Scheme 1. Illustration of the Two Routes Employed for Block Copolymer Functionalization in the Hydrophilic and Hydrophobic Domains

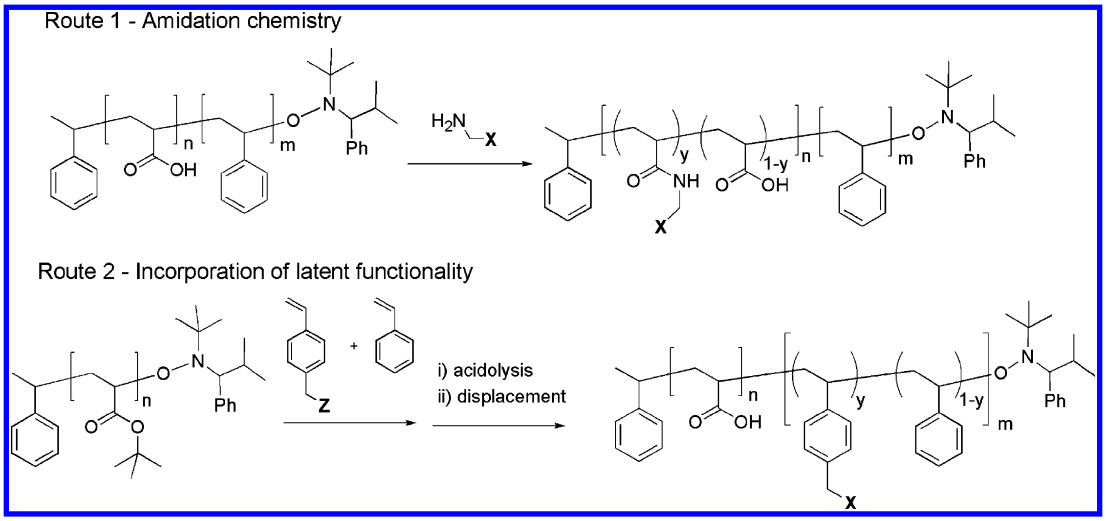

Scheme 2. Preparation of the Amphiphilic Block Copolymer 3, by NMP, Followed by Acidolysis

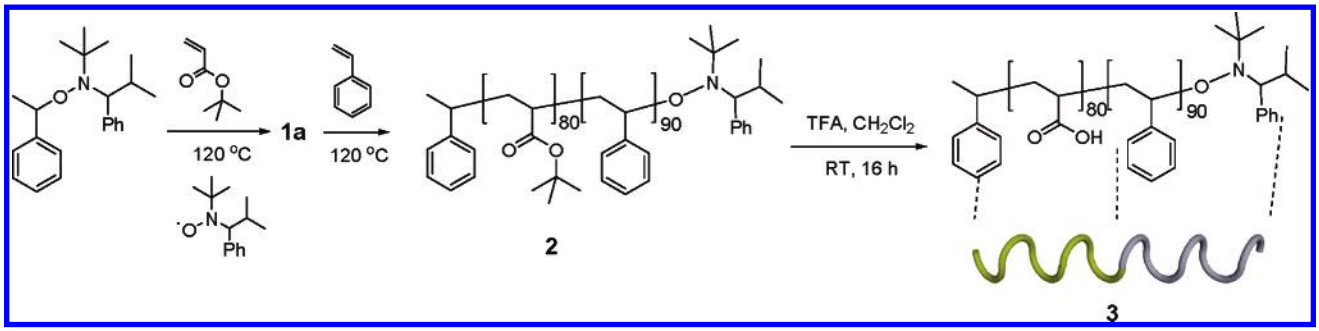

and in the participation in multicomponent cascade reactions.[80,81]

Due to the promise of preparing functionalized nanoparticles in which one or more functional groups (ligands, receptor sites, PNA sequences, etc.) are introduced at specific sites and in controlled numbers, new functionalization routes utilizing Click chemistry were investigated. The general strategy involves the growth of diblock copolymers using nitroxide-mediated polymerization (NMP), subsequent ester deprotection and functionalization to afford the amphiphilic azido or alkynyl functionalized copolymers. Self-assembly and cross-linking of these functionalized copolymers to afford nanoparticles, and their subsequent modification with small molecule chromophores using highly efficient Click chemistry, will be discussed. The ultimate aim is a general strategy for the preparation of well-defined and regioselectively functionalized nanoparticles.

Results and Discussion

To demonstrate the versatility of Click chemistry, two strategies were developed for the regioselective functionalization of micelles and shell cross-linked nanoparticles involving the specific introduction of reactive groups in either their hydrophilic shell or hydrophobic core (Scheme 1). The first approach employs functionalization of the hydrophilic segment of poly(acrylic acid)-*b*-polystyrene, via amidation of a portion of the acrylic acid residues with amino-functionalized azido or alkynyl moieties. This synthetic strategy avoids complicated protection/deprotection schemes, as the alkynyl and azido functionalities are introduced after preparation of the amphiphilic block copolymer. The second route demonstrates the introduction of azido functionality in the hydrophobic segment using a latent functionalized monomer.

Shell Functionalization: Azido and Alkynyl. The preparation of the SCK nanoparticles involved the initial preparation of the amphiphilic diblock copolymer **3**, PAA_{80}-*b*-PS_{90}, by sequential NMP of *tert*-butyl acrylate (**1a**: $M_n = 10600$ g/mol, $M_w/M_n = 1.19$) followed by styrene (**2**: $M_n = 19100$ g/mol, $M_w/M_n = 1.21$).[82] Cleavage of the *tert*-butyl esters upon reaction with trifluoroacetic acid in dichloromethane, as described previously, afforded **3** (Scheme 2),[83] and was confirmed using IR spectroscopy (observed shift of carbonyl

(76) Lewis, W. G.; Green, L. G.; Grynszpan, F.; Radic, Z.; Carlier, P. R.; Taylor, P.; Finn, M. G.; Sharpless, K. B. *Angew. Chem., Int. Ed.* **2002**, *41*, 1053−1057.
(77) Khanetskyy, B.; Dallinger, D.; Kappe, C. O. *J. Comb. Chem.* **2004**, *6*, 884−892.
(78) Harju, K.; Vahermo, M.; Mutikainen, I.; Yli-Kauhaluoma, J. *J. Comb. Chem.* **2003**, *5*, 826−833.
(79) Brik, A.; Muldoon, J.; Lin, Y. C.; Elder, J. H.; Goodsell, D. S.; Olson, A. J.; Fokin, V. V.; Sharpless, K. B.; Wong, C. H. *Chembiochem* **2003**, *4*, 1246−1248.
(80) Ramachary, D. B.; Barbas, C. F. I. *Chem. Eur. J.* **2004**, *10*, 5323−5331.
(81) Appukkuttan, P.; Dehaen, W.; Fokin, V. V.; Van der Eycken, E. *Org. Lett.* **2004**, *6*, 4223−4225.
(82) Benoit, D.; Chaplinski, V.; Braslau, R.; Hawker, C. J. *J. Am. Chem. Soc.* **1999**, *121*, 3904−3920.
(83) Ma, Q. G.; Wooley, K. L. *J. Polym. Sci., Part A: Polym. Chem.* **2000**, *38*, 4805−4820.

Scheme 3. Reagents and Conditions[a]

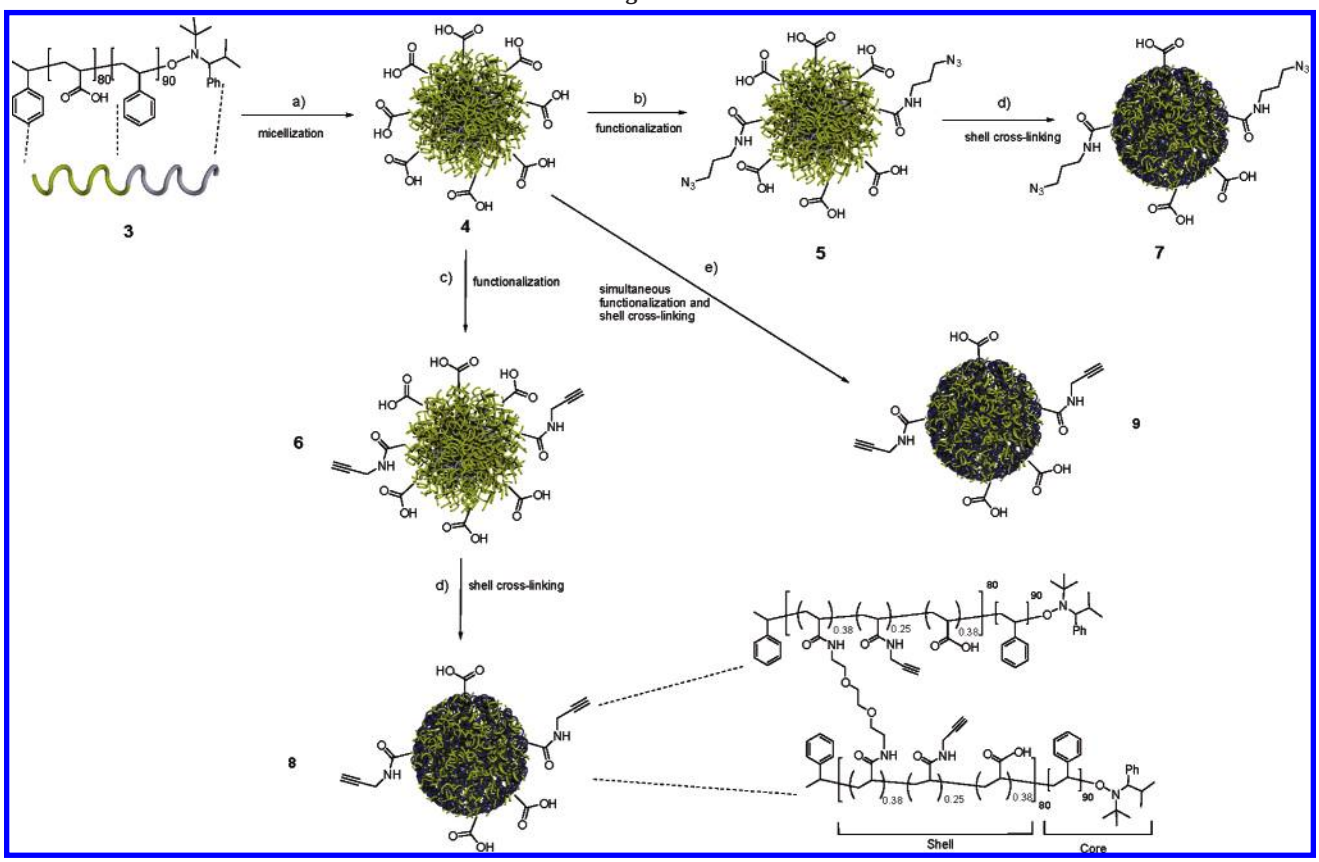

[a] Key: (a) THF, followed by addition of water and dialysis vs water; (b) 3-azidopropylamine (0.25 equiv to acid functionalities), 1-[3′-(dimethylamino)propyl]-3-ethylcarbodiimide methiodide (0.30 equiv to acid functionalities), RT, overnight, followed by dialysis against water; (c) propargylamine (0.25 equiv to acid functionalities), 1-[3′-(dimethylamino)propyl]-3-ethylcarbodiimide methiodide (0.30 equiv to acid functionalities), RT, overnight, followed by dialysis against water; (d) 2,2′-(ethylenedioxy)bis(ethylamine) (0.25 equiv based upon the remaining acid functionalities) 1-[3′-(dimethylamino)propyl]-3-ethylcarbodiimide methiodide (0.50 equiv to remaining acid functionalities), RT, overnight, followed by dialysis against water; (e) propargylamine (0.25 equiv to acid functionalities), 2,2′-(ethylenedioxy)bis(ethylamine) (0.19 equiv to acid functionalities), 1-[3′-(dimethylamino)propyl]-3-ethylcarbodiimide methiodide (0.60 equiv to acid functionalities), RT, overnight, followed by dialysis against water.

stretch from 1728 to 1712 cm^{-1} and disappearance of the *tert*-butyl group signatures at 1392 and 1367 cm^{-1}), NMR spectroscopy (disappearance of *tert*-butyl proton resonances at 1.4 ppm and downfield shift of P*t*BuA backbone protons from 2.4 to 2.5 ppm), and DSC analyses (T_g (**2**) = 47 and 106 °C and T_g (**3**) = 130 and 98 °C) of block copolymers **2** and **3**.

Micelles of narrow size distribution, **4**, composed of the block copolymer PAA_{80}-*b*-PS_{90} **3**, were formed by addition of water to a solution of the polymer in tetrahydrofuran (THF) followed by dialysis against deionized water. Subsequent functionalization was accomplished by condensation reaction of either an azido-[84] or alkynyl-functionalized primary amine with acrylic acid residues along the PAA segments located within the shell of the micelles (0.25 equiv amine-to-acid functionalities), facilitated by 1-[3′-(dimethylamino)propyl]-3-ethylcarbodiimide methiodide (0.30 equiv to acid functionalities) (Scheme 3). After dialysis, azido (**5**) and alkynyl (**6**) shell functionalized micelles were isolated and characterized using dynamic light scattering (DLS) and zeta potential measurements. The calculated concentration of the micelle solution was determined by measurement of the final volume of micelle obtained together with the initial weight of the polymer precursors used.

Table 1. Characterization Data for Micelles 4, 5, and 6 and the Corresponding SCK Nanoparticles 7, 8, and 9

	DLS	AFM		TEM	Zeta	DSC
particle	D_h[a] (nm)	D_{av}[b] (nm)	H_{av}[b] (nm)	D_{av}[c] (nm)	ζ[d] (mV)	T_g[e] (°C)
4	47 ± 3	n.d.	n.d.	n.d.	−42 ± 2	139, 101
5	44 ± 4	n.d.	n.d.	n.d.	−35 ± 3	135, 105
6	47 ± 1	n.d.	n.d.	n.d.	−31 ± 2	144, 96
7	39 ± 2	122 ± 18	8 ± 2	31 ± 6	−27 ± 2	100
8	37 ± 3	104 ± 16	5 ± 1	32 ± 4	−22 ± 2	96
9	38 ± 3	136 ± 34	4 ± 1	34 ± 5	−24 ± 2	98

[a] Number-averaged hydrodynamic diameters of SCKs in aqueous solution by dynamic light scattering. [b] Average heights and diameters of SCKs were measured by tapping-mode AFM, calculated from the values for ca. 150 particles. [c] Average diameters of SCKs were measured by TEM, calculated from the values for ca. 150 particles. [d] Zeta potential, from 16 determinations of 10 data sets. [e] Glass transition temperatures, taken as the midpoint of the inflection tangent upon the third heating scan.

The partially functionalized micelles **5** and **6** exhibited little or no change in hydrodynamic diameter (D_h) by DLS analysis (Table 1), relative to the micelle precursor, **4**. However, a decrease in charge from zeta potential measurements was observed and can be attributed to the decrease in concentration of carboxylic acid groups upon amide formation. In addition, IR spectroscopic analysis of micelles **5** and **6** demonstrated a shift of the carbonyl band and the formation

(84) Carboni, B.; Benalil, A.; Vaultier, M. *J. Org. Chem.* **1993**, *58*, 3736−3741.

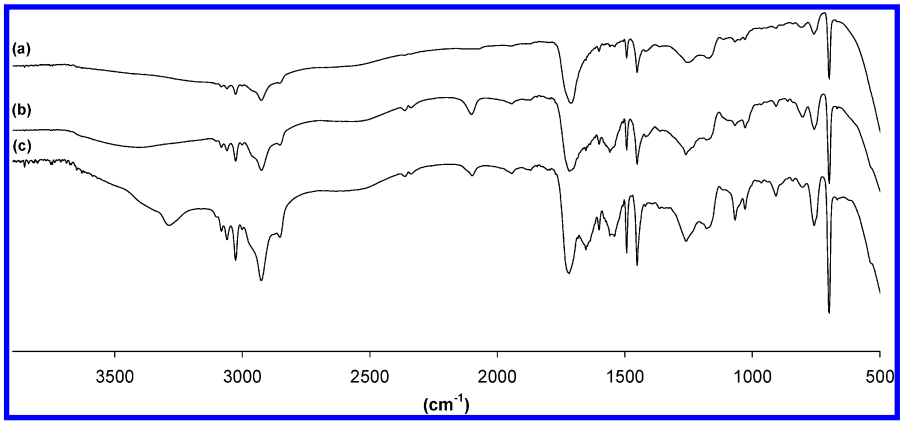

Figure 1. IR spectra (NaCl) of (a) nonfunctionalized micelle, **4**; (b) azido-functionalized micelle, **5**, and (c) alkynyl-functionalized micelle, **6**, *y*-axis % transmittance (arbitrary units).

of amide bands (I and II) at ca. 1650 and 1560 cm^{-1} as well as characteristic absorptions of azido and alkynyl groups at ca. 2100 and at 2110 and 3300 cm^{-1}, respectively (Figure 1).

Click-functionalization experiments were also performed on the amphiphilic (PAA-*b*-PS) block copolymers prior to micellization, in a THF:H_2O mix utilizing the same amidation chemistry. However, this route was not favored and instead the functionalization of a stock solution of PAA-*b*-PS micelles (**4**) provided a homogeneous nanoassembly starting point from which versatility of chemistry could be investigated, using either an azido- or alkynyl-substituted amine (**5** and **6**, respectively).

The micelles (**5** and **6**) were then cross-linked using amidation chemistry by activating a fraction of the remaining carboxylic acid groups, with 1-[3′-(dimethylamino)propyl]-3-ethylcarbodiimide methiodide (0.50 equiv based upon the remaining acid functionalities) followed by reaction with 2,2′-(ethylenedioxy)bis(ethylamine) (0.25 equiv based upon the remaining acid functionalities) overnight at ambient temperature (Scheme 3).[85] The Click-functionalized nanoparticles, **7** and **8**, were then purified by dialysis to remove the urea byproducts and afford **7** and **8** with concentrations ca. 0.23 mg/mL. Each micelle was cross-linked at a calculated mean cross-linking density of 37.5%, based on the stoichiometry of amine functional groups of the diamine cross-linker to the remaining carboxylic acid groups from the functionalized PAA-*b*-PS block copolymers.

The size and shape of the SCKs (**7** and **8**) were measured in the solid state (adsorbed) by atomic force microscopy (AFM) and transmission electron microscopy (TEM) and in solution using DLS and zeta potential measurements (Table 1). Significantly, TEM analysis gave nanoparticle diameters (D_{av}) which were similar to the respective hydrodynamic diameters obtained from DLS analysis. The small heights (H_{av}) of nanoparticles **7**−**9** indicate that significant deformation from the spherical shape observed in solution is occurring upon absorption onto the mica AFM surface. Furthermore, the larger diameter values (D_{av}) obtained from AFM measurements, in comparison to those from TEM, indicate greater deformation of the particles on the hydrophilic mica surface, the substrate for AFM characterization, as opposed to the hydrophobic carbon surface, the substrate for TEM characterization. The lateral sizes of the particles (D_{av}) by AFM analysis are also distorted due to the finite size of the AFM tip; therefore, the particle diameters obtained by TEM analysis were considered to be of greater precision and were used for further analyses.

Zeta potential measurements, as determined by electrophoretic light scattering, were negative (Table 1). These data indicate negative charges on the surfaces of the nanoparticles and micelle precursors. The micelle zeta potential values were generally more highly negative than were those values measured for their nanoparticle counterparts, thus supporting the synthetic transformation occurring in the surface layer of the micelle upon consumption of carboxylates during transformation to the nanoparticle.

Differential scanning calorimetry (DSC) of micelles **5** and **6** showed two transitions (T_g's), at around 140 and 100 °C, indicating phase separation into PS and PAA domains. Upon cross-linking, the nanoparticles displayed only one T_g, (ca. 100 °C), by DSC analysis, corresponding to the PS core. Characterization of the entire composition of the SCKs by solution NMR spectroscopy was not possible because the nanoparticles were invisible in solution (DMSO-d_6) spectra. IR spectroscopic analysis of a lyophilized portion of the SCKs, **7**−**9**, confirmed the presence of the characteristic absorbances for the azido and alkynyl functionalities at ca. 2100 and 2105 cm^{-1}, respectively, and also displayed new signals attributable to the ethylene glycol cross-linker at ca. 1100 cm^{-1}.

An alternative route to Click-functionalized nanoparticles is the simultaneous reaction of the carboxylic acid groups with both the cross-linker and Click-functionalized amine. This allows for concurrent cross-linking and functionalization as demonstrated in route e) in Scheme 3, to afford the nanoparticle **9** in a single step. As illustrated in Table 1, there is no apparent difference in size, shape, or distribution of nanoparticles formed using a single-step or two-step procedure (cf. nanoparticle **8** versus **9**). Figure 2 shows representative TEM images and histograms of the D_{av} values and corresponding distributions for nanoparticles **8** and **9**.

Core Functionalization: Azide. The absence of functional groups, such as carboxylic acid moieties, in the

(85) Thurmond, K. B., II; Kowalewski, T.; Wooley, K. L. *J. Am. Chem. Soc.* **1997**, *119*, 6656−6665.

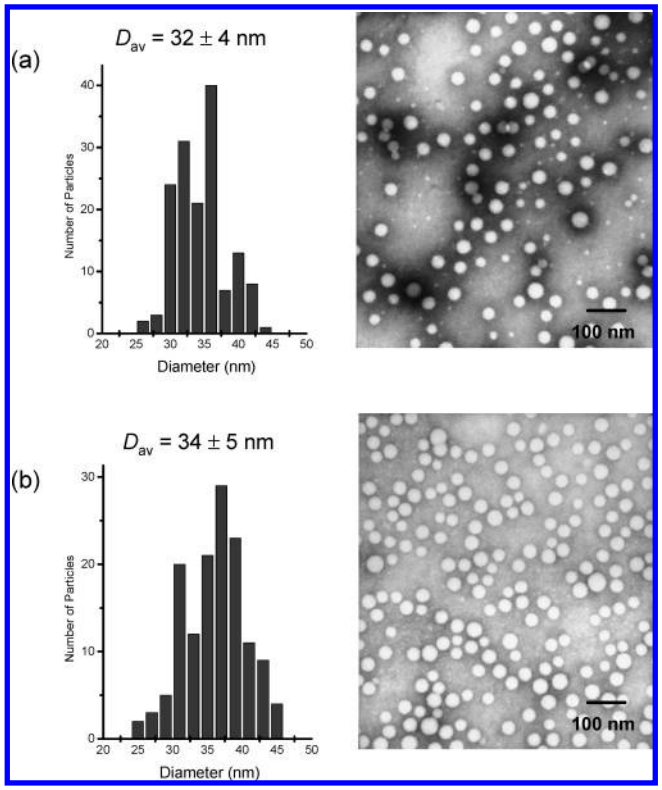

Figure 2. Representative TEM images of nanoparticles (a) **8** prepared in two steps and (b) **9** prepared in a single step. Average diameters are shown with the corresponding distribution and a representative image. Samples were stained with phosphotungstic acid, drop-deposited onto a carbon-coated copper grid, and allowed to dry under ambient conditions.

hydrophobic core of either micelles or nanoparticles necessitated a different strategy to introduce the Click reactive groups within the core domain. By incorporation of a functionalized styrenic monomer in the PAA-*b*-PS block copolymer synthesis, functionality could be introduced into the hydrophobic domain of the amphiphilic block copolymer. It has been demonstrated that chloro or bromo groups can serve as latent azido functional groups and efficiently converted to azido groups by reaction with sodium azide.[86] Thus, a poly(*tert*-butyl acrylate) homopolymer **1b** (M_n = 6800 g/mol, M_w/M_n = 1.16) was prepared using NMP and then further extended by the polymerization of a mixture of styrene and 4-vinyl benzyl chloride (20 mol % relative to styrene) to afford P*t*BuA$_{50}$-*b*-[PS-*co*-PSCl]$_{70}$, **10** (M_n = 16900 g/mol, M_w/M_n = 1.19). Removal of the *tert*-butyl esters was achieved by reaction with trifluoroacetic acid in dichloromethane, as described for **2** (Scheme 4). This reaction sequence yielded an amphiphilic block copolymer, PAA$_{50}$-*b*-[PS-*co*-PSCl]$_{70}$, **11**, which could then undergo supramolecular assembly in water to afford micelles, **12**.

The displacement of the chloro groups for azides in micelle **12** was achieved by addition of DMSO (ca. 5 vol %) and reaction with excess NaN_3 (5.0 equiv) at room temperature. Dialysis against water removed excess NaN_3 and NaCl to afford the functionalized micelle, PAA$_{50}$-*b*-[PS-*co*-PS(N_3)]$_{70}$, **13** (Scheme 5). The successful introduction of azido groups was confirmed by the appearance of a characteristic absorbance at ca. 2100 cm^{-1} in the IR spectrum of **13**. In addition, comparison of NMR spectra, in DMSO-d_6, of lyophilized samples of micelles **12** and **13** indicated complete conversion of the chloro group to an azide by an upfield shift of the resonance attributable to the methylene group from ca. 4.45 to 4.55 ppm.

It should be noted that the order in which functionalization and deprotection of the polymers was performed is critical to the success of the procedure. The azido-functionalized block polymer P*t*BuA-*b*-[PS-*co*-PS(N_3)] can be prepared by reaction of the chloro precursor, **10**, with NaN_3 overnight in DMF at ambient temperature.[87] However, attempts to perform the subsequent ester deprotection to afford the amphiphilic block copolymer PAA-*b*-[PS-*co*-PS(N_3)] led to a loss in azido functionality, as evidenced by IR spectroscopic analysis. Thus, the deprotection of the *tert*-butyl ester groups must be performed prior to introduction of the azido functionality.

The azido core-functionalized SCK nanoparticles, **14**, were formed by intramicellar cross-linking of approximately 50% of the acrylic acid residues (Scheme 5). Amide bond formation was confirmed by IR spectroscopy with the introduction of amide I and II bands at ca. 1640 and 1560 cm^{-1}, and the azido functionality was still present and visible at ca. 2100 cm^{-1}. As was observed for the shell-functionalized micelles, a decrease in D_h, by DLS analysis, was observed on cross-linking, as was a decrease in negative surface charge density, as measured by zeta potential analysis. In addition, AFM and TEM imaging indicated that the core-functionalized nanoparticle **14** appeared to flatten on the AFM surface, leading to a significant deviation from a spherical shape, as was discussed for the shell-functionalized derivatives (Table 2).

It should be noted that the Click-functionalized micelles and nanoparticles, especially the azido derivatives, displayed limited shelf lives (1−2 months), when stored at room temperature on the bench, compared to their nonfunction-

Scheme 4. Synthetic Route for the Preparation of the Functionalized Amphiphilic Block Copolymer 11, by NMP, Followed by Acidolysis

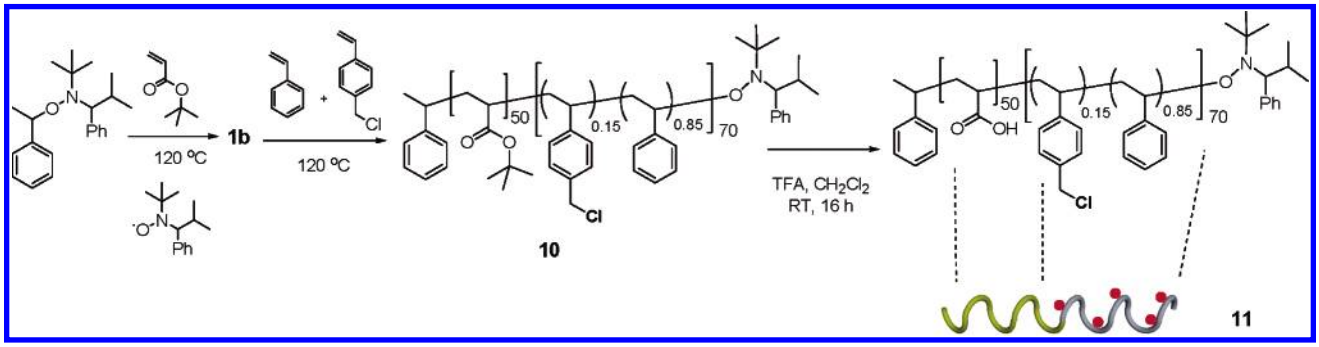

Scheme 5. Reagents and Conditions[a]

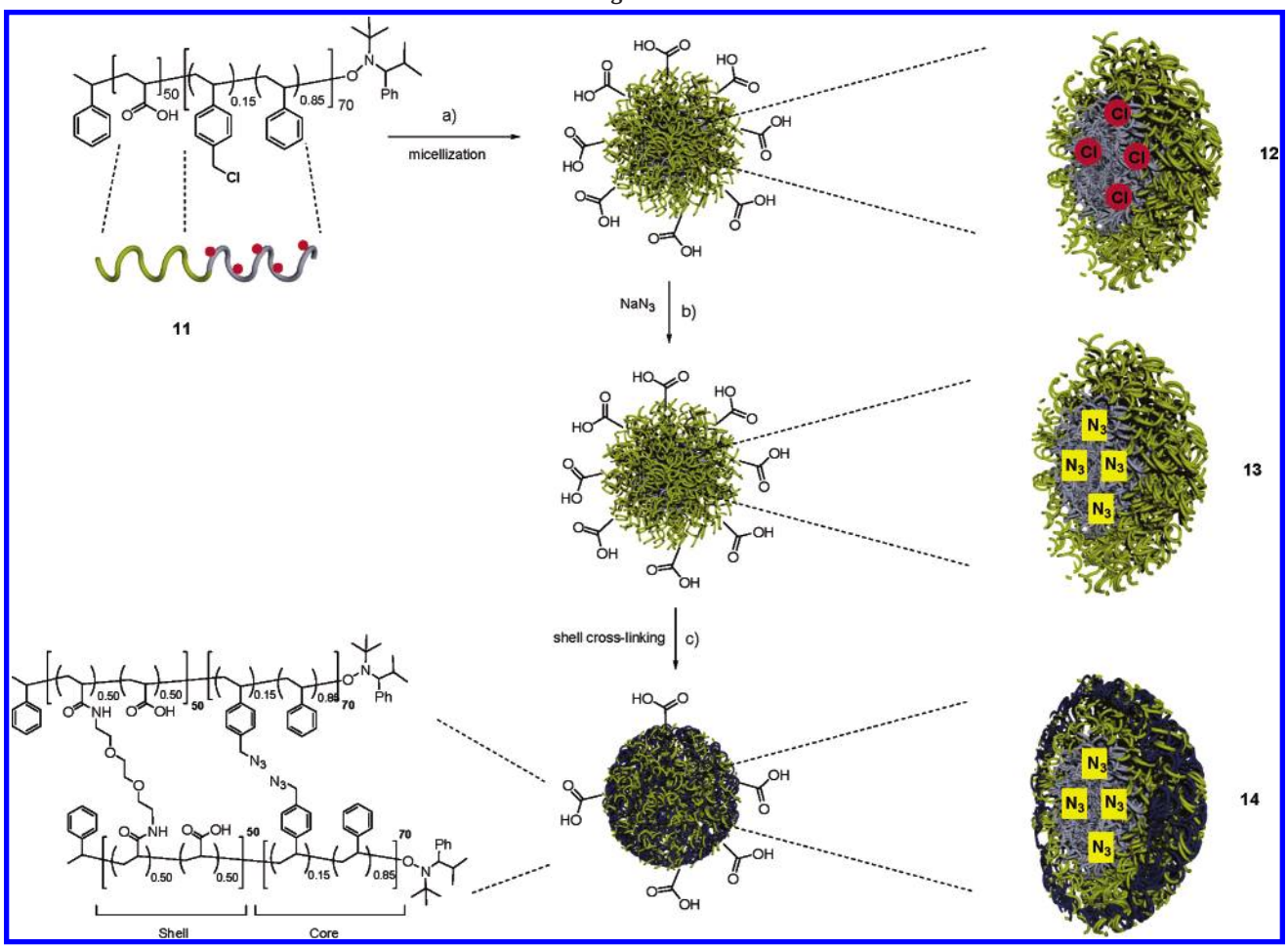

[a] Key: (a) THF, followed by addition of water and dialysis against water; (b) 5.0 equiv of NaN_3, DMSO (ca. 5 vol %), RT, 3 d, followed by dialysis against water; (c) 2,2′-(ethylenedioxy)bis(ethylamine) (0.25 equiv based upon the acid functionalities), 1-[3′-(dimethylamino)propyl]-3-ethylcarbodiimide methiodide (0.50 equiv to acid functionalities), RT, overnight, followed by dialysis against water.

Table 2. Characterization Data for Micelles 12 and 13 and SCK Nanoparticle 14

	DLS	AFM		TEM	zeta	DSC
particle	D_h[a] (nm)	D_{av}[b] (nm)	H_{av}[b] (nm)	D_{av}[c] (nm)	ζ[d] (mV)	T_g[e] (°C)
12	28 ± 2	n.d.	n.d.	n.d.	−49 ± 3	97, 137
13	27 ± 1	n.d.	n.d.	n.d.	−46 ± 3	98, 148
14	22 ± 2	111 ± 18	3 ± 1	20 ± 1	−33 ± 2	93

[a] Number-averaged hydrodynamic diameters of SCKs in aqueous solution by dynamic light scattering. [b] Average heights and diameters of SCKs were measured by tapping-mode AFM, calculated from the values for ca. 150 particles. [c] Average diameters of SCKs were measured by TEM, calculated from the values for ca. 150 particles. [d] Zeta potential, from 16 determinations of 10 data sets. [e] Glass transition temperatures, taken as the midpoint of the inflection tangent upon the third heating scan.

alized precursors.[88] By DLS analysis, aggregation appeared to be occurring over time, which skewed the distribution of hydrodynamic diameters resulting in an increase in polydispersity ($D_{h,volume}/D_{h,number}$, see Supporting Information).

Core Functionalization: Alkynyl. With use of the chloro-functionalized amphiphilic block copolymer **11**, unsuccessful attempts were made to introduce alkynyl functionality via a slight modification to the methods described by Endo and co-workers.[89] Attempts to convert the chloro functionality into an alkynyl group in the hydrophobic precursor P*t*BuA-*b*-[PS-*co*-PSCl] (**10**) were successful (**15**); however, the subsequent deprotection of the *tert*-butyl ester groups using TFA and other deprotection strategies led to a loss of alkynyl functionality (see Supporting Information). In contrast to the azido chemistry, the inability to displace the benzylic chloride groups with propargyl alcohol in the presence of PAA prohibited the introduction of the alkynyl group after establishment of the amphiphilic block copolymer. Therefore, the functionalization of the hydrophobic domain with alkynyl groups requires further study and alternative routes are currently under development.

Click Reactions. The availability of the azido and alkynyl groups within the nanoparticle shell and core toward copper-catalyzed triazole formation was evaluated using alkynyl- and azido-functionalized fluorescent dyes. Recently, there has been increasing interest in the synthesis and functionalization of fluorescent dyes for utilization in Click chemistry. Indeed, azido and/or alkynyl fluorescent dyes have been

(86) Alvarez, S. G.; Alvarez, M. T. *Synthesis* **1997**, 413−414.
(87) Speers, A. E.; Adam, G. C.; Cravatt, B. F. *J. Am. Chem. Soc.* **2003**, *125*, 4686−4687.
(88) Huang, H. Y.; Kowalewski, T.; Remsen, E. E.; Gertzmann, R.; Wooley, K. L. *J. Am. Chem. Soc.* **1997**, *119*, 11653−11659.
(89) Kishi, K.; Ishimaru, T.; Ozono, M.; Tomita, I.; Endo, T. *J. Polym. Sci., Part A: Polym. Chem.* **2000**, *38*, 35−42.

Scheme 6. Reagents and Conditions[a]

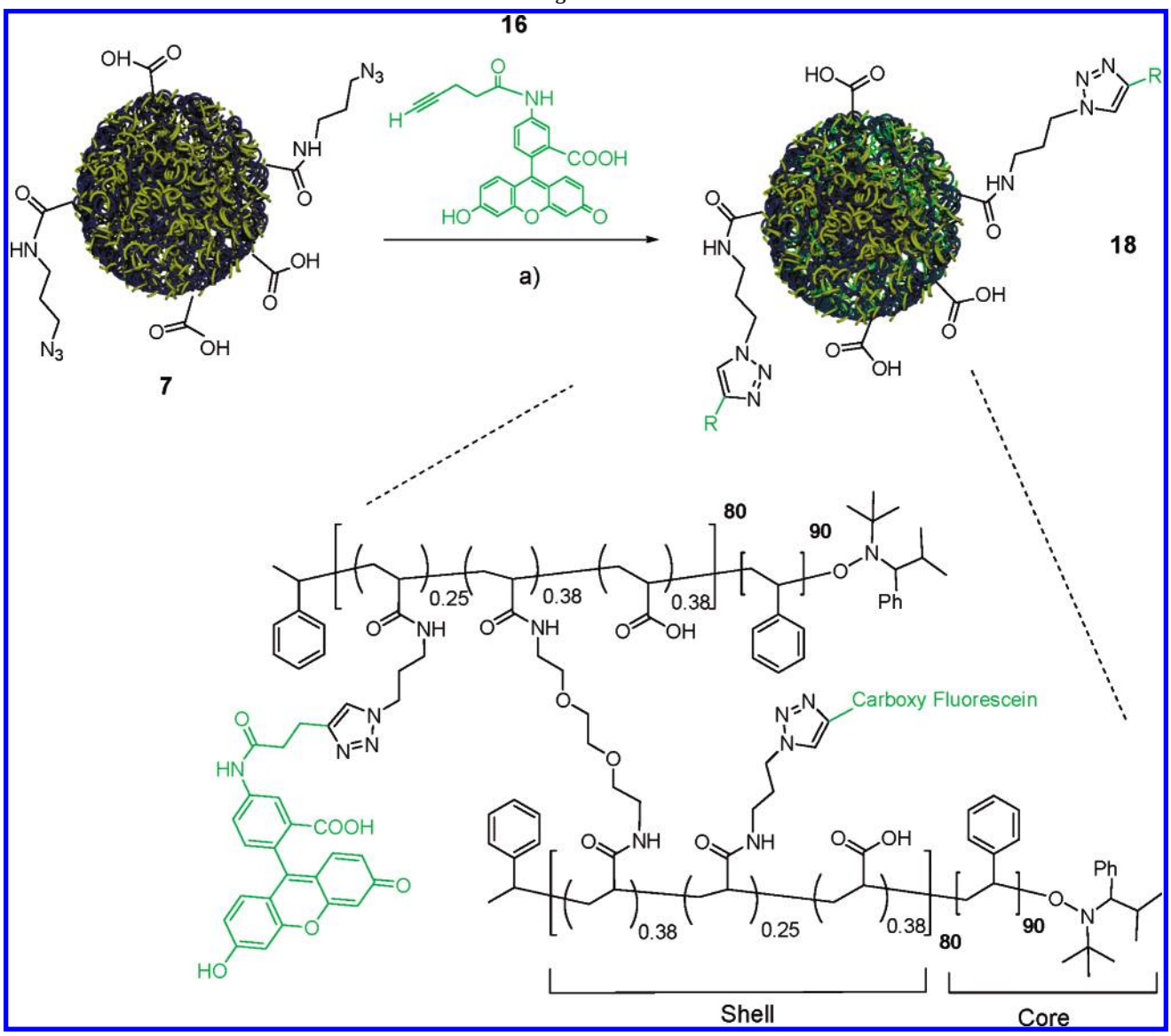

[a] Key: (a) $CuSO_4 \cdot 5H_2O$ (0.25 equiv), sodium ascorbate (5 wt % solution in water, 0.50 equiv), **16** (1.11 equiv to azido functionality), RT, 2 d, followed by dialysis against pH 7.3 phosphate buffered saline, 10 d.

demonstrated to have applications in catalysts discovery and screening,[90] fluorescence quenching,[91,92] fluorescent labeling of DNA,[74] and virus capsid proteins,[93] and also as chemoselective fluorogenic probes.[94] Tirrell and co-workers recently demonstrated the high efficiency of this Click chemistry in the detection and presentation of noncanonical amino acids in cell surface proteins which were previously believed to be silent.[95] Such high chemical efficiency, combined with the sensitivity of fluorophores, was therefore expected to allow for demonstration of the accessibility of the incorporated azide and alkynyl moieties with accurate quantification.

Shell Click Reactions. The nanoparticles carrying Click reactive functionalities in the hydrophilic shell, **7** and **8**, were allowed to react with either an alkynyl- or azido-functionalized fluorescein dye (**16** or **17**), synthesized by modification of literature procedures,[93,96,97] in the presence of a Cu(I) catalyst that was generated in situ from $CuSO_4 \cdot 5H_2O$ (0.25 equiv) and sodium ascorbic acid (0.50 equiv as a 5 wt % aqueous solution). The reactions were allowed to proceed for 2 days at ambient temperature and were then purified by exhaustive dialysis against sodium phosphate buffered saline at pH 7.3, to afford labeled nanoparticles **18** and **19** (Schemes 6 and 7).

Although the chemistry is straightforward, confirmation of the covalent coupling versus physical absorption of dye molecules required the use of multiple characterization techniques. The successful fluorescent functionalization of

(90) Lewis, W. G.; Magallon, F. G.; Fokin, V. V.; Finn, M. G. *J. Am. Chem. Soc.* **2004**, *126*, 9152−9153.
(91) Crabtree, R. H. *Chem. Commun.* **1999**, 1611−1616.
(92) Loch, J. A.; Crabtree, R. H. *Pure Appl. Chem.* **2001**, *73*, 119−128.
(93) Wang, Q.; Chan, T. R.; Hilgraf, R.; Fokin, V. V.; Sharpless, K. B.; Finn, M. G. *J. Am. Chem. Soc.* **2003**, *125*, 3192−3193.
(94) Zhou, Z.; Fahrni, C. J. *J. Am. Chem. Soc.* **2004**, *126*, 8862−8863.
(95) Link, A. J.; Vink, M. K. S.; Tirrell, D. A. *J. Am. Chem. Soc.* **2004**, *126*, 10598−10602.
(96) Crisp, G. T.; Gore, J. *Tetrahedron* **1997**, *53*, 1505−1522.
(97) Deiters, A.; Cropp, T. A.; Mukherji, M.; Chin, J. W.; Anderson, J. C.; Schultz, P. G. *J. Am. Chem. Soc.* **2003**, *125*, 11782−11783.

Scheme 7. Reagents and Conditions[a]

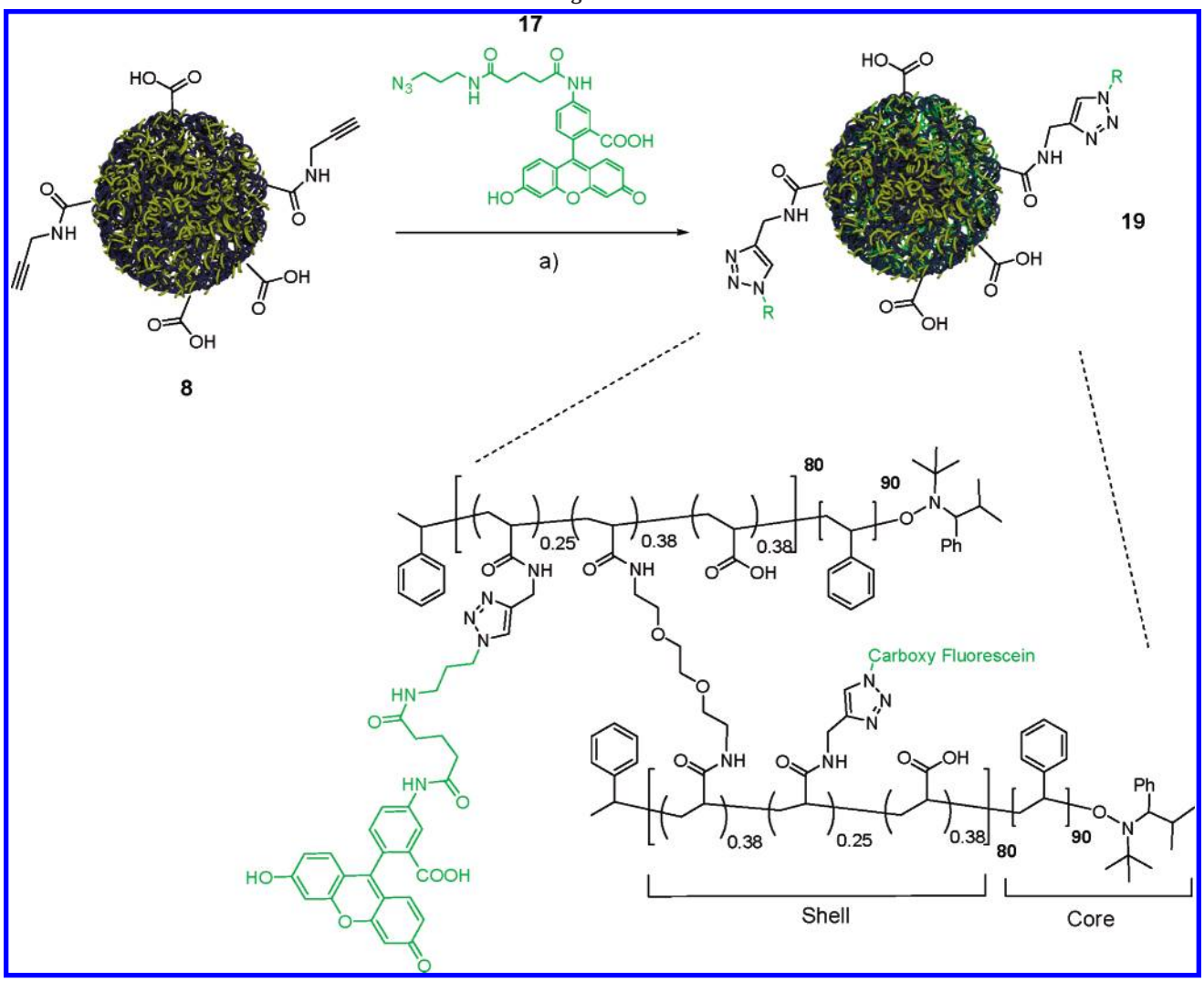

[a] Key: (a) $CuSO_4 \cdot 5H_2O$ (0.25 equiv), sodium ascorbate (5 wt % solution in water, 0.50 equiv), **17** (1.11 equiv to alkynyl functionality), RT, 2 d, followed by dialysis against pH 7.3 phosphate buffered saline, 10 d.

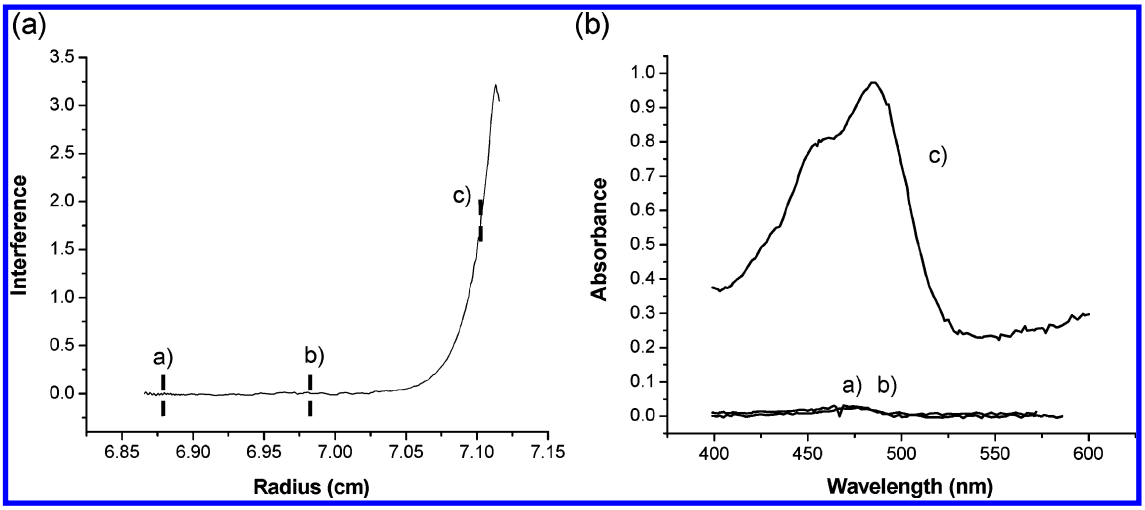

Figure 3. Sedimentation equilibrium profile (5000 rpm) collected using an interferometry detector for the nanoparticle **19** (left panel) and corresponding absorption spectra, recorded at different radial positions (right panel) across the sedimentation equilibrium profile: a) top, b) middle, and c) bottom.

the nanoparticles **18** and **19** was best confirmed by analytical ultracentrifugation (AU) in combination with UV−vis absorption spectra collected in the range of 400−600 nm at different radial positions (top, middle, and bottom of the cell) across the sedimentation equilibrium (SE) profile (Figure 3). Any free dye in solution would be uniformly distributed throughout the solution volume while the nanoparticles sediment and thus are depleted from the meniscus along with any dye molecules covalently bound to them. From Figure 3, it is apparent that an absorption maximum (ca. 500 nm)

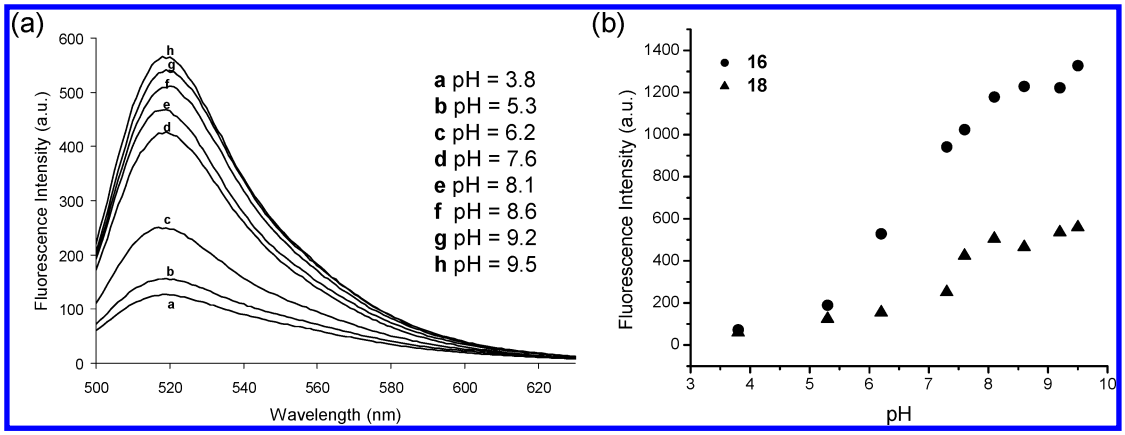

Figure 4. (a) Fluorescence emission spectra (excitation wavelength $\lambda_{ex} = 488$ nm) from **18** at different pH values in a 50 mM sodium phosphate buffered saline. (b) Comparison plots of fluorescence emission intensities from nanoparticle **18** and free dye **16** (at $\lambda_{em} = 517$ nm) versus pH. Each sample solution was prepared independently from a stock solution at ca. 0.23 mg/mL.

was observed only near the bottom of the cell and negligible free dye was present in other areas of the cell. These AU results confirmed the successful isolation of SCKs in aqueous solutions having dye molecules attached covalently via Click chemistry, and retaining no free dye.

The amounts of dye Clicked to the nanoparticles were quantified using UV−vis spectroscopy by application of the methods of Andrisano and co-workers[98] based on calculation of the first derivative UV−vis spectrophotometric analyses. For each of the nanoparticles **18** and **19**, the concentration of dye was found to be ca. 2.50×10^{-6} M, which correlated with the theoretical concentration of Click reactive groups in the polymer chains (2.56×10^{-6} M) and demonstrates the quantitative nature of the Click reaction and its insensitivity to the relative placements of the azido and alkynyl groups.

Fluorescence spectroscopy, performed as a function of pH, illustrated the effect of the covalent attachment of fluorescein within the carboxylic acid-containing SCK nanoparticle shell and the resulting unique environment that is created, as observed by enhanced quenching of fluorescein emission. Figure 4 highlights this effect for **18**, which exhibits reduced fluorescence emission intensity at all pH levels, compared to the control experiment for free fluorescein dye. The observed intensity reduction of the emission spectrum of **18** may be attributed to the shielding effect of the poly(acrylic acid) shell upon attachment of the dye within the nanoparticle compared to **16**, the free dye molecule in solution. As Cu(II) is an established fluorescence quencher, control studies were performed using a nonfunctionalized nanoparticle subjected to Click conditions with **16** and identical dialysis conditions. The resulting solutions did not demonstrate quenching of the dye emission spectrum and thus it can be concluded that any remaining Cu(II) salts do not cause the quenching observed in Figure 4 and instead it can be attributed to local charge effects.

Techniques that measured particle size and surface charge density were rather insensitive to the introduction of the fluorophores; however, minor changes were observed (Table 3). A slight increase in nanoparticle size (D_h) was observed in aqueous solution by DLS analysis, following the cycloaddition reaction while there was no discernible effect on the surface charge density as quantified by zeta potential determination.

Table 3. Comparison of Characterization Data for SCKs 7 and 8 before Click and SCKs 18 and 19 after Click Reaction with a Fluorescein Dye

particle	DLS D_h[a] (nm)	AFM H_{av}[b] (nm)	TEM D_{av}[c] (nm)	Zeta ζ[d] (mV)
7	39 ± 2	8 ± 2	31 ± 6	−27 ± 2
8	37 ± 3	5 ± 1	32 ± 4	−22 ± 2
18	44 ± 2	16 ± 3	34 ± 4	−28 ± 2
19	43 ± 2	15 ± 3	36 ± 4	−23 ± 2

[a] Number-averaged hydrodynamic diameters of SCKs in aqueous solution by dynamic light scattering. [b] Average heights and diameters of SCKs were measured by tapping-mode AFM, calculated from the values for ca. 150 particles. [c] Average diameters of SCKs were measured by TEM, calculated from the values for ca. 150 particles. [d] Zeta potential, from 16 determinations of 10 data sets.

By TEM analysis, the nanoparticle diameter values (D_{av}) were comparable, before and after Click reaction. However, AFM imaging indicated that the attachment of the fluorescein dye in nanoparticles **18** and **19** altered the interaction of the nanoparticle with the mica surface significantly, which resulted in larger heights (H_{av}) for the fluoresceinated nanoparticles **18** and **19** compared to their azido- and alkynyl-functionalized precursors, **7** and **8**, respectively. Figure 5 shows representative AFM images of nanoparticles **7** and **18** to illustrate the increased particle height upon conjugation of the dye molecule. The significantly greater difference in particle height vs D_h or D_{av} suggests alteration in nanoparticle-to-substrate interactions upon modification of the SCK nanoparticle surface chemistry. Such ability to tune SCK nanoparticle shape adaptability[99] and surface interactions[100] is a key area of future development.

In addition, the fluorescently labeled nanoparticles **18** and **19** were lyophilized to afford solid-state samples, which were then analyzed using IR and NMR spectroscopic techniques. IR spectroscopy highlighted the disappearance of the azido or alkynyl functional groups in the nanoparticles and showed

(98) Andrisano, V.; Bartolini, M.; Bertucci, C.; Cavrini, V.; Luppi, B.; Cerchiara, T. *J. Pharm. Biomed. Anal.* **2003**, *32*, 983−989.

(99) Huang, H. Y.; Kowalewski, T.; Wooley, K. L. *J. Polym. Sci., Part A: Polym. Chem.* **2003**, *41*, 1659−1668.

(100) Qi, K.; Ma, Q. G.; Remsen, E. E.; Clark, C. G., Jr.; Wooley, K. L. *J. Am. Chem. Soc.* **2004**, *126*, 6599−6607.

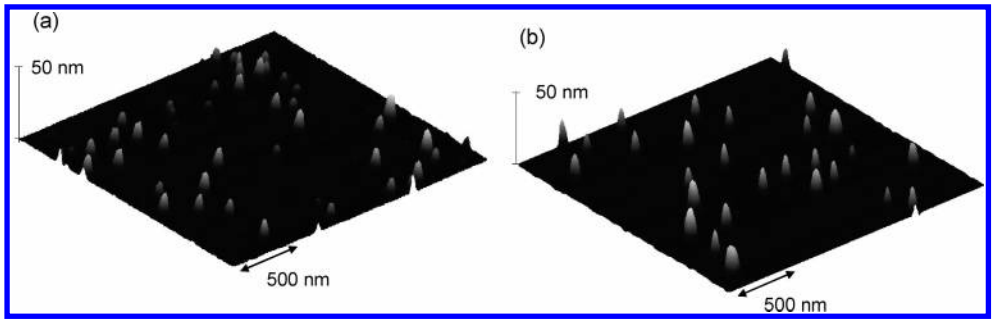

Figure 5. Representative tapping-mode AFM images of nanoparticles (a) **7** and (b) **18**. Samples were prepared by drop deposition onto freshly cleaved mica and allowed to dry under ambient conditions.

Scheme 8. Reagents and Conditions[a]

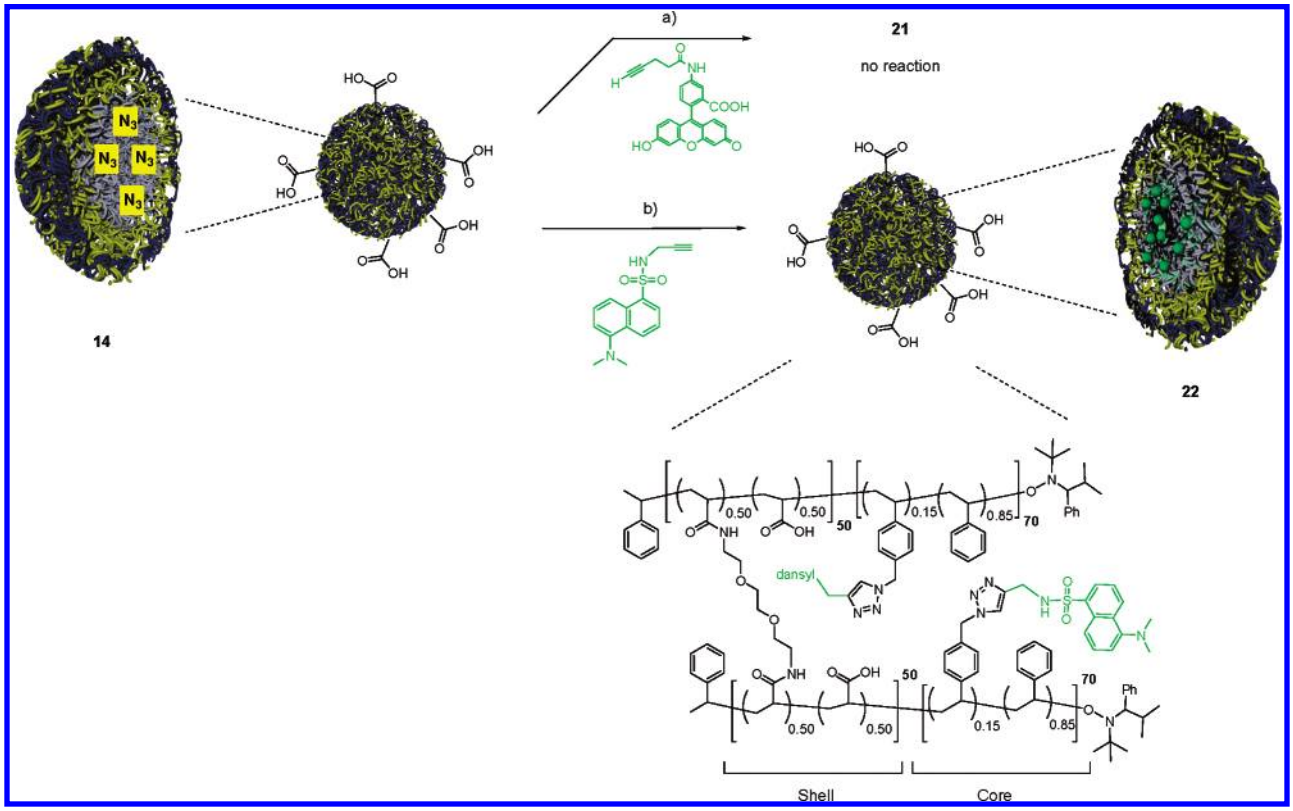

[a] Key: (a) $CuSO_4 \cdot 5H_2O$ (0.25 equiv), sodium ascorbate (5 wt % solution in water, 0.50 equiv), **16** (1.11 equiv to azido functionality), RT, 2 d, followed by dialysis against pH 7.3 phosphate buffered saline, 10 d; (b) dialysis into a 1:1 THF:H_2O mix for 3 d, then addition of $CuBr(PPh_3)_3$ (0.1 equiv), and DIPEA (1.0 equiv), **20**[97,101] (1.11 equiv to azido functionality), RT, 2 d, followed by dialysis against a 1:1 THF:buffered H_2O mix for 10 d, and then dialysis against pH 7.3 phosphate buffered saline, 4 d.

the appearance of new absorbances attributable to the fluorescent dye molecule. NMR spectroscopy (DMSO-d_6) revealed resonances characteristic of the dye molecule and triazole moiety but not the polymer signals, as would be expected for a cross-linked particle (see Supporting Information). The aryl protons of the fluorescein dye are visible at 8.25, 7.74, 7.14, and 6.62−6.45 ppm. The multiplet at 6.62−6.45 ppm integrates to 7 proton resonances and this has been attributed to the 6 aryl protons of the dye and also a single-proton resonance attributable to the triazole proton. Resonances that may be assigned to the aliphatic linker of the dye molecule are also visible at ca. 2.78 and 2.55 ppm, although accurate integration is difficult, due to their proximity to residual protons in the DMSO solvent.

Core Click Reactions. In consideration of functionalization of the nanoparticle core, a number of unique issues must be considered. Unlike the shell, which is a swollen hydrogel, the core is hydrophobic and for the covalent attachment to occur, reagents must transverse the shell layer and core−shell interface while being soluble in the hydrophobic nanoenvironment of the core. To address these multiple issues, the reaction of core-functionalized nanoparticles was investigated under both aqueous and organic conditions with either a hydrophilic or hydrophobic alkynyl dye (Scheme 8).

(a) Aqueous Media. Initial experimental results indicated that the Click reaction between the alkynyl-functionalized fluorescein and the azido side chain groups within the SCK nanoparticle cores failed to occur under aqueous conditions, as determined by DLS, TEM, and AFM analysis. Upon exhaustive dialysis, UV−vis spectroscopy revealed that there was essentially no dye present in the nanoparticle solution and this observation was confirmed by AU analysis (Figure 6). Lyophilization of a sample of **21** and subsequent NMR

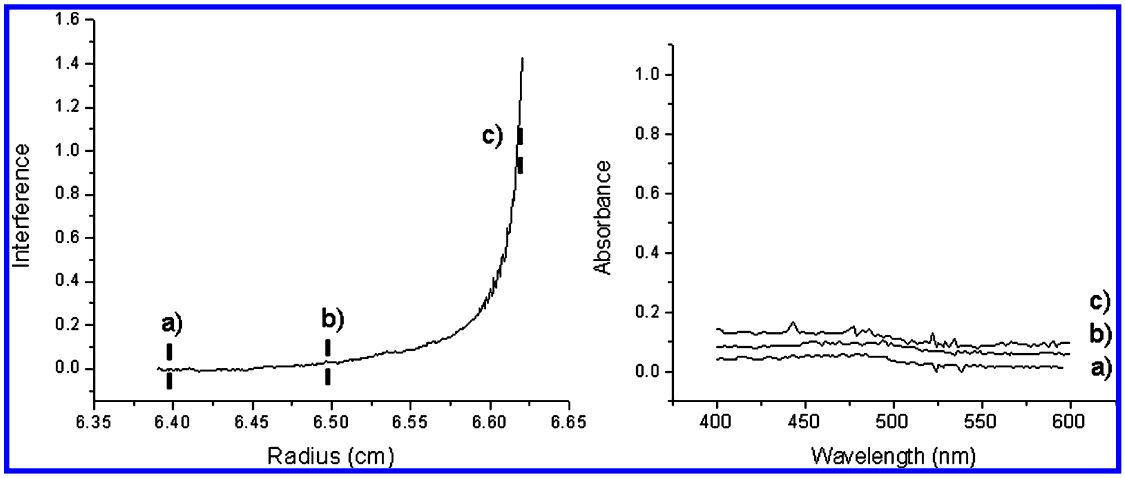

Figure 6. Sedimentation equilibrium profile (5000 rpm) collected using an interferometry detector for the nanoparticle **21** and corresponding absorption spectra, recorded at different radial positions, a) top, b) middle, and c) bottom, across the sedimentation equilibrium profile.

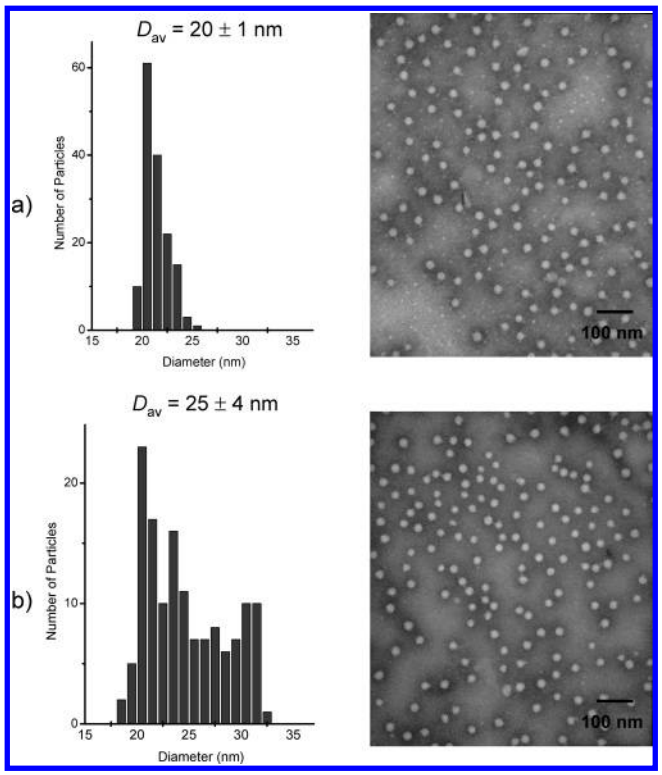

Figure 7. TEM images of nanoparticles a) **14** and b) **22**. Average diameters are shown with the corresponding distribution and a representative image. Samples were stained with phosphotungstic acid, drop-deposited onto a carbon-coated copper grid, and allowed to dry under ambient conditions.

and IR spectroscopic analyses also indicated the presence of nonreacted azido functionality and showed no evidence of resonances attributable to fluorescein. Attempts to conduct the Click reaction of a hydrophobic dansyl derivative with functional groups present in the hydrophobic domain of the SCK nanoparticle were unsuccessful under standard aqueous reaction conditions due to the insolubility of the dye.

(b) Organic Media. It has been demonstrated that the copper-catalyzed cycloaddition reaction between azides and alkynes can also be conducted in organic solvents in the presence of $CuBr(PPh_3)_3$ and an organic base.[52] The synthetic strategy was modified, therefore, to apply the alkynyl-functionalized dansyl derivative, **20**,[97,101] to the core Click functionalization of SCKs nanoparticle in 1:1 H_2O/THF. The core of **14** was swollen by dialysis for 3 days in a 1:1 THF: H_2O solution, and then the Click reaction was allowed to proceed for 2 days at ambient temperature, followed by purification by exhaustive dialysis (initially against a 1:1 mixture of sodium phosphate buffered saline at pH 7.3 and THF and then against buffered H_2O) to afford the dansyl-functionalized nanoparticle, **22**. DLS analysis of **22** indicated that the nanoparticles exhibited a slight increase in D_h upon functionalization with the dansyl derivative ($D_h = 29 \pm 5$ nm), while both TEM and AFM analyses showed little or no difference in particle diameter or height before and after functionalization (Figure 7). AU analysis confirmed association of the dye molecule with the nanoparticle (see Supporting Information). Both IR and NMR spectroscopic analyses showed absorbances and resonances attributable to the dansyl fluorescent dye and the loss of the azido functionality, thus supporting successful conjugation of the dansyl dye within the nanoparticle core.

Conclusions

Synthetic strategies for the preparation of novel azido- and alkynyl-functionalized micelles and SCK nanoparticles were developed and their viability as Click-readied nanoscale substrates validated. With use of covalent condensation or displacement reactions to conduct chemical modification of amphiphilic block copolymers, in combination with supramolecular assembly, regioselective placement of Click reactive functionalities was achieved.

The introduction of the Click reactive groups in both the hydrophilic and hydrophobic domain of the amphiphilic core−shell materials provides a route for versatile functionalization of these well-defined nanostructures. In this initial demonstration, we have shown that the functionalized nanoparticles could be fluorescently tagged in either the core or the shell domain utilizing the copper(I)-catalyzed cycloaddition of azides and alkynes. It was further demonstrated that the reaction conditions and dye molecule employed for the cycloaddition could be tailored to match the local nanoenvironment within these structures. Importantly, the covalent attachment versus sequestration of hydrophilic, pH-

(101) Bolletta, F.; Fabbri, D.; Lombardo, M.; Prodi, L.; Trombini, C.; Zaccheroni, N. *Organometallics* **1996**, *15*, 2415−2417.

sensitive fluoresceins was confirmed by AU analysis and UV−vis spectroscopy.

Given the ever expanding growth and interest in the fields of Click chemistry and nanomaterials, the preparation of these novel nanoparticles allows for the merging of these disciplines and also enables the labeling of nanomaterials with biologically active ligands, among other moieties. The straightforward introduction of bioactive molecules will allow for tracking and detection of these nanoparticles in both in vivo and in vitro conditions. These azido- and alkynyl-functionalized micelles also have the potential for the development of new cross-linking techniques utilizing Click chemistry.

Acknowledgment. This work is based upon work supported by the National Science Foundation under the Nanoscale Interdisciplinary Research Team (NIRT) program Grant number 0210247 and also Grant number 0451490. Acknowledgment is also made to the donors of the Petroleum Research Fund, administered by the ACS, and the MRSEC program (DMR-05-20415) for partial support of this research. M.J.J. was supported by a Chemistry-Biology Interface Program Fellowship under an NIH Training Grant No. NIHNRSA 5-T32-GM08785-0. R.K.O'R. was partially supported by a Research Fellowship from the Royal Commission for the Exhibition of 1851. Mr. G. Michael Veith, of the Washington University Department of Biology, is gratefully acknowledged for TEM analysis. Ms. Lucy Li (IBM) and Mr. Teddie Magbitang (IBM) are thanked for assistance with thermal and GPC analysis, respectively. Mr. Jeffery L. Turner is thanked for schematic drawings of SCK nanoparticles.

Supporting Information Available: Detailed experimental procedures and characterization data for all polymers, micelles, and nanoparticles. This material is available free of charge via the Internet at http://pubs.acs.org.

CM051047S